

## NATURAL CONVECTION HEAT TRANSFER FROM HORIZONTAL AND SLIGHTLY INCLINED PLATE-FIN HEAT SINKS

Ilker Tari<sup>1</sup>, Mehdi Mehrtash

Mechanical Engineering Department, Middle East Technical University, 06800  
Ankara, Turkey

### Abstract

Natural convection from plate-fin heat sinks in both horizontal and slightly inclined from horizontal orientations is studied for the inclination angles of  $\pm 60^\circ$ ,  $\pm 75^\circ$ ,  $+80^\circ$ ,  $\pm 85^\circ$ ,  $\pm 90^\circ$  from the vertical. A set of correlations is obtained for both upward (–) and downward (+) facing horizontal cases. The correlations are tested for validity by using large sets of experimental data from literature. By varying the direction of gravitational acceleration for several upward and downward inclinations, the phenomenon is investigated for the purpose of determining the flow structures forming in and around the heat sinks. The chimney flow structures forming in the upward facing horizontal case are investigated. The extents of validity of the horizontal case correlations for the average Nusselt number are investigated by modifying the dimensionless body force terms with the sine of the inclination angle. It is observed that the modified correlations are valid in ranges, from  $-60^\circ$  to  $-90^\circ$  (upward) and  $+80^\circ$  to  $+90^\circ$  (downward). A complete set of Nusselt number correlations covering all possible inclination angles is suggested and shown to be accurate with less than 20% error for the cases with fin spacing values close to the determined optima.

**Keywords:** Plate-fin array; Inclined heat sink; Natural convection; Electronics cooling; Correlation.

### Nomenclature

|              |  |
|--------------|--|
| $d$          | Base plate thickness, mm   |
| $g$          | Gravitational acceleration, $\text{m/s}^2$   |
| $Gr$         | Grashof number, $Gr = g\beta\Delta TS^3/\nu^2$   |
| $Gr'$        | Modified Grashof number, $Gr' = Gr(H/L)^{m_1}(S/H)^{m_2}$  |
| $Gr'_v$      | Modified Grashof number for vertical heat sink,<br>$Gr'_v = [g\beta\Delta TS^4]/[\nu^2(LH)^{0.5}]$                                 |
| $Gr'_{up,h}$ | Modified Grashof number for upward facing horizontal heat sink,<br>$Gr'_{up,h} = [g\beta\Delta TS^3](H/L)^{0.5}(S/H)^{0.38}/\nu^2$ |
| $h$          | Average heat transfer coefficient, $\text{W}/(\text{m}^2 \text{K})$  |
| $H$          | Fin height, mm   |
| $k$          | Thermal conductivity of air, $\text{W}/(\text{m K})$   |
| $L$          | Fin length, mm   |
| $Nu_S$       | Nusselt number based on $S$ , $Nu_S = (hS)/k$  |
| $Pr$         | Prandtl number   |
| $Q_c$        | Convection heat transfer rate from heat sink, W  |
| $Q_{in}$     | Power supplied to heater plate, W  |
| $Q_r$        | Radiative heat transfer rate from heat sink, W   |

<sup>1</sup> Corresponding author. Tel.: +90 312 2102551; fax: +90 312 2102536. E-mail address: itari@metu.edu.tr (I. Tari).

|            |   |
|------------|---|
| $Ra_S$     | Rayleigh number based on $S$ , $Ra_S = Gr Pr = g\beta\Delta TS^3/(v\alpha)$ |
| $S$        | Fin spacing, mm   |
| $S_{opt}$  | Optimum fin spacing, mm   |
| $t$        | Fin thickness, mm   |
| $T_w$      | Average base wall temperature, °C   |
| $\Delta T$ | Base-to-ambient temperature difference, K                                   |
| $W$        | Heat sink width, mm   |

#### Greek Symbols

|          |   |
|----------|---|
| $\alpha$ | Thermal diffusivity, $m^2/s$                                    |
| $\beta$  | Volumetric thermal expansion coefficient, $1/K$                 |
| $\theta$ | Angle of inclination with respect to vertical position, degrees |
| $\nu$    | Kinematic viscosity, $m^2/s$                                    |

### 1. Introduction

Electronics cooling by natural convection with the help of finned heat sinks is a common practice due to its ease of implementation, powerless operation and high reliability. Heat sinks with parallel arrangement of rectangular cross section plate fins on a flat base are used preferably in vertical or upward facing horizontal orientations in order to obtain higher natural convection rates [1]. In certain scenarios, however, one may be forced to consider plate-fin heat sinks in inclined orientations. This may be either due to the rotation of the heat sink as a result of a rotation of the device, or due to some system related constraint, *e.g.*, the lack of available space on the side and top surfaces of the electronic box or the lack of vertical and horizontal surfaces in the design. Hence, for practical purposes, there is certainly a need for investigating inclined plate-fin heat sinks. For example, when natural convection with vertical plate-fin heat sinks was suggested as a viable solution for cooling of flat panel displays with high power components [2] and of laptop computers [3], the major concern was how to handle the situation if the device is operated when the heat sink is inclined as a result of the inclination of the screen. Despite its importance, there are only two experimental studies in literature dealing with inclined orientations: The first one, by Starner and McManus [1], deals only with upward  $45^\circ$  inclination. The second one, by Mittelman et al. [4], deals with downward inclination angles between  $60^\circ$  and  $90^\circ$ .

Recently in Tari and Mehrtash [5], we have numerically studied plate-fin heat sinks inclined from the vertical, proposing a new set of correlations for vertical heat sinks, and then showing its validity (after modifying the equations with cosine of the inclination angle) for inclinations in the range of  $-60^\circ$  to  $+80^\circ$ .

We conjecture that the left out ranges around horizontals, namely from  $-60^\circ$  to  $-90^\circ$  (upward facing) and  $+80^\circ$  to  $+90^\circ$  (downward facing) may be explained by modifying the respective horizontal correlations with sine of the inclination angle. The aim of the present study is to test this conjecture. Towards this aim, we obtain natural convection heat transfer correlations for the upward and downward horizontals, and then modify them by multiplying the body force with the sine of the inclination angle from the vertical. At the end of the study, we obtain a full set of correlations that is valid in all inclination angles. To be consistent with our previous work [5], all angles are measured from the vertical.

In order to test the conjecture, we need correlations for both downward and upward orientations of the heat sink. The downward facing horizontal case is studied only by Mittelman et al. [4][6] who did not suggest a correlation for heat transfer

rates. Thus we need to obtain our own correlation for the downward case. The upward facing horizontal case, on the other hand, has been investigated in several works. As classified in [7] there are mainly two groups of experimental works: Starner-McManus-Harahap (S-M-H) [1][8] and Leung-Probert-Shilston (L-P-S) [9-14]. A recent detailed review can be found in Dogan and Sivrioglu [15]. Among the experimental works, Starner and McManus [1], Harahap and Setio [7], Harahap and McManus [8] and Leung and Probert [13] suggest generalized correlations for the natural convection heat transfer rate from upward facing horizontal heat sinks. The results of these studies and the suggested correlations, however, do not agree well with each other; the differences in results are attributed (in [7]) to the differences between the experimental set-ups of the two groups. The lack of consistent correlations prompted us to formulate our own correlations for the horizontal case.

To be able to obtain the correlations, effects of all geometric parameters of the heat sink on the natural convection heat transfer rate should be studied in detail. Following our approach in [5], by varying the heat sink length ( $L$ ), fin height ( $H$ ), the fin spacing ( $S$ ), and the heat input ( $Q_{in}$ ), we determined the average convective and radiative heat transfer rates dissipated from the heat sink after performing series of simulations.

Our numerical model was previously validated at the vertical orientation [5] and used for inclined orientations from vertical in both formal [5] and practical [16] settings by varying the orientation of the gravitational acceleration vector. In this paper, following the same approach for creating the effect of inclination, we study inclined orientations from horizontal.

## 2. Numerical Model and Method

The model assembly includes an aerated concrete insulation on the backside of a heater plate and a heat sink attached to the front of the heater. The heat sink geometry is shown in upward facing horizontal orientation in Fig. 1. The assembly is placed in an air filled cubical room of 3 m sides with walls that are maintained at uniform 20 °C. In the analysis (with ANSYS [17]), steady state solutions are obtained by using the zero-equation-turbulence model with initial ambient air temperature of 20 °C. Air is taken as an ideal gas at atmospheric pressure. No slip boundary condition is used for all surfaces. There is no contact resistance between solid surfaces. A more detailed description of the numerical model, the model validation processes (for a flat plate and a vertical fin array), and the effects of different parameters on the heat transfer rate in the vertical case were previously given in [5].

By changing the orientation of the gravitational acceleration vector, any inclination of the heat sink can be created. In Fig. 2(a), the vertical model is shown together with the gravitational acceleration vector pointing towards the heat sink on the wall creating the net effect of an upward facing horizontal heat sink that is shown in Fig. 2(b). The downward facing horizontal heat sink is shown in Fig. 2(c). Since throughout the present study, the previously validated vertical model is used without any modification (except  $g$  direction changes), there is no need for a further validation study.

A non-conformal mesh structure with a very fine grid around the cooling assembly and a coarse grid for the rest of the room is employed. Grid independence is achieved by examining three different grid densities with 1685832, 2834264 and 4077608 cells, and then selecting the medium density mesh, i.e., the one with 2834264 cells, as it yields results matching to those of the fine mesh. ANSYS solver [17] is used for solving the continuity, momentum and thermal energy equations for

air as an ideal gas and the heat conduction equation within the solids. To handle the radiative heat transfer, the surface-to-surface radiation model of ANSYS is used for all surfaces by taking emissivities of 0.2 and 0.9 respectively for the aluminum heat sink and the aerated concrete insulation.

For the upward and downward facing horizontal orientations of the heat sink, heat sink parameters are varied over their respective practical ranges. As a result, we obtained enough data to generalize the dependency of natural convection heat transfer rates to heat sink geometric parameters.

### 3. Results and Discussions

Steady state simulations are performed for a range of heater power values and for ranges of geometric parameters of the heat sink. Two separate sets of data are collected: (i) large amount of data in the upward and downward facing horizontal orientations of the heat sink for obtaining horizontal case correlations, and (ii) inclined case data at various angles for a heat sink with a fixed fin spacing. Sections 3.1 and 3.2 are for the horizontal cases and Sections 3.3 and 3.4 are for the inclined cases.

#### 3.1. Upward and downward facing horizontal orientations

In upward and downward facing horizontal orientations of the heat sinks, in order to collect enough data for generalization and to be able to resolve the parametric dependencies, all of the important parameters are varied within ranges that are suitable for electronics cooling applications. While keeping the width ( $W$ ) and base thickness ( $d$ ) of the heat sink constant at 180 mm and 5 mm, and the fin thickness ( $t$ ) constant at 3 mm, we try the same values of the other parameters in [5] for the upward and downward horizontal cases:

- 250 and 340 mm for the heat sink length  $L$ ,
- 25, 50, 75, 100 and 125 W for the heat input  $Q_{in}$ ,
- 11, 12, 13, 14, 15, and 16 for the number of fins spanning the width corresponding to the fin spacing ( $S$ ) values of 14.7, 13.09, 11.75, 10.62, 9.64, and 8.8 mm, respectively.
- 5, 15, and 25 mm for the fin height  $H$ .

The collected horizontal case data is analyzed to examine the parametric dependencies and the flow structures. The first parametric analysis is done for the fin spacing and optimum fin spacing values for both of the horizontal orientations are obtained by finding the values minimizing the base temperature as it is discussed in [15]. The optimum fin spacing values are within 8.8-9.9 mm and 12.3-13.9 mm ranges for the downward and upward facing horizontal cases, respectively (Table 1). These results confirm the differences in phenomena for the downward and upward facing horizontal orientations.

#### 3.2. Horizontal case correlations

In [5], considering buoyancy driven airflow in a channel between two consecutive fins of a vertical plate-fin heat sink, five dimensionless groups were obtained from the governing equations, which led to the following definition of a modified Grashof number:

$$Gr' = Gr(H/L)^{m_1}(S/H)^{m_2} \quad (1)$$

where  $Gr = g\beta\Delta TS^3/\nu^2$ .

The average Nusselt number based on  $S$ , which should be a function of  $Gr'$  and  $Pr$  takes the following simple form:

$$Nu_S \equiv \frac{hS}{k} = C(Gr'Pr)^n \quad (2)$$

For the vertical orientation of the heat sink, we have set the powers in Eq. (1) as  $m_1 = 1/2$  and  $m_2 = 1$ , making  $Gr'_v = [g\beta\Delta TS^4]/[\nu^2(LH)^{0.5}]$ . The power in Eq. (2),  $n$ , has been determined to be

$$n = \begin{cases} 1/2 & \text{for } Gr'Pr < 250 \\ 1/3 & \text{for } 250 < Gr'Pr < 10^6 \end{cases} \quad (3)$$

together with respective  $C$  values of 0.0929 and 0.2413 that are determined from the best fit of the data in [5].

In the horizontal case, however,  $m_1$  and  $m_2$  need to be modified in order to change the fin height dependence of  $Nu_S$ . Our analysis with two-variable identification maximizing squared correlation coefficient ( $R^2$ ) of the fit of the simulation data suggests that both  $m_1$  and  $m_2$  should be zero for the downward horizontal case, making the right hand side variable in (2)  $Ra_S = Gr Pr = g\beta\Delta TS^3/(\nu\alpha)$ . For the upward horizontal case, however,  $m_2$  should be selected as 0.38 while keeping  $m_1$  as 0.5. With these new powers, we need to define a new modified Grashof number for the upward horizontal case,  $Gr'_{up,h} = [g\beta\Delta TS^3](H/L)^{0.5}(S/H)^{0.38}/\nu^2$ .

These new  $m_1$  and  $m_2$  values make the data for three different fin heights (5, 15 and 25 mm) and two different heat sink lengths (250 and 340 mm) to fall on to a single power curve with the best  $R^2$  in each orientation. As a consequence of changing  $m_1$  and  $m_2$ , the power  $n$  in Eq. (2) takes different values for each horizontal case.

In order to obtain a correlation for the downward horizontal case,  $Nu_S$  is plotted against  $Ra_S$  using the entire downward horizontal data set in Fig. 3. The best fit is obtained according to the form in Eq. (2) as

$$Nu_S = 0.0149 Ra_S^{0.5} \quad (4)$$

The squared correlation coefficient ( $R^2$ ) of the fit is 0.9332. When the present data are taken as the truth, the absolute relative error varies between 0.08% and 16.73% with an average of 5.96%. In Fig. 3., the same form is used also for the data from Mittelman et al. [4] and it is observed that the fit is also good for their data set with an absolute relative error of  $\pm 10.9\%$ . This indicates that Eq. (4) is applicable to the Mittelman et al. [4] data.

For the upward horizontal case,  $Nu_S$  is plotted against  $Gr'_{up,h}Pr$  in Fig. 4. The best power fit in the form of Eq. (2) is obtained as

$$Nu_S = 0.0915 (Gr'_{up,h}Pr)^{0.436} \quad (5)$$

The  $R^2$  of the fit is 0.9666. When the present data values are taken as true values, the absolute relative error varies between 0.03% and 14.31% with an average of 4.32%. In Fig. 4, the data from Starner and McManus is also plotted and is observed to be compatible with Eq. (5) with an absolute relative error of  $\pm 27.6\%$ . Considering that the usual reported accuracy for similar correlations in the literature is an order of magnitude, Eq. (5) can be considered very accurate.

To further show the accuracy of Eq. (5), the data from S-M-H [18] and L-P-S [14] groups are also used. Four sets of data for upward facing horizontal heat sinks that were provided by Harahap [18] are plotted in Figure 5 using the form of Eq. (5). Especially, the data sets named as H3 and H4 show very good agreement while H1 and H2 show acceptable agreement. The geometric parameters of the aluminum heat sinks are given together with the absolute relative error taking the experimental data as the true values are presented in Table 2. Also in Figure 5, the rest of the Harahap

data [18] (S-M-H) and the data obtained from Leung and Probert [14] (L-P-S) are plotted.

From Fig. 5 and Table 2, the following observations can be made after marking the data with less than ~20% error in boldface:

- While S-M-H data agrees very well with the present data (and the associated correlation form) only for H1-H4 data sets, the agreement of L-P-S data within the range of the present data is very good.
- It seems that S-M-H group did not investigate the  $S$  dependence in detail. Since in the present study, the investigated range of  $S$  is larger than the ones in S-M-H data, the agreement is better for the data from larger  $S$ .
- L-P-S group investigated the  $S$  dependence. For  $L=170$  mm, the better agreement with the present data is in  $S=9-21$  mm range, the best agreement corresponding to  $S=15$  mm which is close to the  $S_{opt}$  value obtained here.
- Overall, the suggested form for correlation, Eq. (5) is accurate within 20% accuracy for most of the S-M-H and L-P-S data for the cases with similar  $S$  values to the ones investigated in the present study.

An important phenomenon for natural convection with upward facing horizontal plate finned heat sinks is the chimney structure forming on top of the heat sink. This phenomenon was originally investigated by Harahap and McManus [8] using smoke for visualization. Airflow inside horizontal plate finned heat sinks follows the channels among the parallel fins after entering the channels from both ends of the heat sink. In the middle of the sink the streams coming from both ends collide and forms the chimney structure. In Fig 6., speed contours for the heat sinks of 25, 15 and 5 mm fin heights are presented. The midlines of the central channels are the centers of the chimney structures where the buoyancy driven upward flow is the strongest. The chimney structures for the fin heights of 15 and 5 mm are shown in Fig. 7 from which it is observed that the chimney thickness is less for the  $H=5$  mm fins. There is also a very important difference in flow inside the channels: for the 5 mm fin height, the blue region towards the middle of the channels that is expanding towards the outer channels in Fig. 6 corresponds to the recirculation region observed in Fig. 7. Due to this region in which longitudinal vortices form, about 1/3 of the heat sink area is not effectively used. According to Fig. 7, these longitudinal vortices contribute to the chimney at the center of the fin thus forming a thinner chimney. The important result of these observations is that 5 mm fin height is not a good choice for the considered heat load and other geometric parameters.

This is the first time such structures are observed in plate-finned heat sinks with the help of numerical simulations. Since the final result of this phenomenon is a significant decrease in the heat transfer performance of the heat sink, there is certainly a need for further numerical and experimental investigations.

### 3.3 Upward and downward small inclinations from the horizontal

The numerical data obtained from the simulations for each inclination angle are post-processed to obtain average surface temperatures ( $T_w$ ), heat convection rates ( $Q_c$ ) and radiative transfer rates ( $Q_r$ ) for three fin heights (5, 15 and 25 mm) and for three heater input powers (25, 75 and 125 W). Since the flow structures in upward and downward inclinations of the heat sink show considerable differences, a large amount of data is collected and the upward and downward directions are separately discussed.

For the upward facing close to horizontal inclinations of the heat sink, Eq. (5) is modified by multiplying the dimensionless body force related term ( $Gr'_{up,h} Pr$ ) with the sine of the inclination angle; the following equation is obtained

$$Nu_S = 0.0915 (Gr'_{up,h} Pr \sin \theta)^{0.436} \quad (6)$$

In Figure 8, Eq. (6) is plotted together with the simulation data obtained in the  $-90^\circ < \theta < -60^\circ$  interval. As the inclination angle decreases towards  $-60^\circ$  the accuracy of Eq. (6) decreases. The absolute percent relative errors are 8%, 5.79%, 5.12%, 4.13%, 3.76%, 4.22%, and 2.81% respectively for  $-60^\circ$ ,  $-65^\circ$ ,  $-70^\circ$ ,  $-75^\circ$ ,  $-80^\circ$ ,  $-85^\circ$ , and  $-90^\circ$  inclination angles from the vertical.

For the downward facing plate-fin heat sink case, we previously obtained a correlation covering  $0^\circ < \theta < +80^\circ$  interval [5]. Outside of that range, as an inclined case data, only the  $+85^\circ$  data is left. The modification is again done with the sine of the inclination angle giving the following relation:

$$Nu_S = 0.0149 (Ra_S \sin \theta)^{0.5} \quad (7)$$

The present data for  $+85^\circ$  and  $+80^\circ$  inclination angles are shown in Figure 9 together with the curve for Eq. (7). The suggested correlation, Eq. (7) agrees very well with the  $+85^\circ$  data with  $\pm 6.1\%$  error. Since the  $+80^\circ$  data was already covered with the correlation in [5], we do not expect a good agreement with Eq. (7). In fact, the error for the  $+80^\circ$  data is  $\pm 17.8\%$ . Only available data from Mittelman et al. [4] for comparison are for the downward horizontal ( $+90^\circ$ ) and  $+80^\circ$  data. As expected, Mittelman et al.  $+80^\circ$  data shows  $\pm 15.2\%$  error, similar to the present data, while Mittelman et al.  $+90^\circ$  data agrees well with Eq. (7) ( $\pm 10.9\%$  error) (see Fig. 8).

### 3.4 Complete correlation set for all inclinations

The correlations suggested in Tari and Mehrtash [5] for the  $-60^\circ < \theta < +80^\circ$  interval are

$$Nu_S = 0.0929 (Gr'_v Pr \cos \theta)^{0.5} \quad \text{for } Gr'_v Pr \cos \theta < 250 \quad (8)$$

$$Nu_S = 0.2413 (Gr'_v Pr \cos \theta)^{1/3} \quad \text{for } 250 < Gr'_v Pr \cos \theta < 10^6 \quad (9)$$

where  $Nu_S \equiv (hS)/k$  is the Nusselt number based on fin spacing  $S$ ,  $Pr$  is the Prandtl number,  $Gr'_v = [g\beta\Delta TS^4]/[\nu^2(LH)^{0.5}]$  is the first modified Grashof number, and  $\theta$  is the inclination angle measured from the vertical.

The correlation suggested for the upward facing  $-90^\circ < \theta < -60^\circ$  interval is

$$Nu_S = 0.0915 (Gr'_{up,h} Pr \sin \theta)^{0.436} \quad \text{for } Gr'_{up,h} Pr \sin \theta < 5000 \quad (10)$$

where  $Gr'_{up,h} = [g\beta\Delta TS^3](H/L)^{0.5}(S/H)^{0.38}/\nu^2$  is the second modified Grashof number.

The correlation suggested for the downward facing  $+80^\circ < \theta < +90^\circ$  range is

$$Nu_S = 0.0149 (Ra_S \sin \theta)^{0.5} \quad \text{for } Ra_S \sin \theta < 1.8 \times 10^4 \quad (11)$$

where  $Ra_S = Gr Pr = g\beta\Delta TS^3/(\nu\alpha)$  is the Rayleigh number based on fin spacing.

## 4. Conclusion

For the inclined cases, the previously uncovered inclination angle ranges of  $-90^\circ < \theta < -60^\circ$  and  $+80^\circ < \theta < +90^\circ$  are investigated. A set of horizontal correlations is suggested. These correlations are shown to be very accurate in predicting heat transfer rates using the available horizontal data from the literature. Since the accuracies of the correlations suggested in the previous literature are only within an order of magnitude even for the well investigated upward facing horizontal case, the achieved accuracies with the present correlations is a noteworthy improvement.

When considered together with our former set of correlations, our correlations cover all possible inclination angles. The complete set of correlations is given by Equations (8)-(11). The accuracy of the complete set of correlations is shown to be very high. For heat sinks with optimal fin spacing, even when compared to all of the experimental data, errors of the correlations remain within the  $\pm 20\%$  interval.

There are several possible applications of the suggested correlations such as natural convection cooling and water management of PEM fuel cells [19][20], electronics cooling with foam heat sinks [21], plate fins embedded in phase change materials [22][23]. When other fin geometries are considered plate fins are advantageous for natural convection because of the possibility of providing a larger heat transfer surface for example compared to pin fins [24], while addition of pin fins between adjacent plate fins may improve heat transfer characteristics for forced convection [25].

### Acknowledgment

The authors thank Amos Ullmann and Filino Harahap for the experimental data provided for comparison. M. Mehrtash acknowledges the financial support provided by TUBITAK through BIDEB 2215 scholarship program.

### References

- [1] K.E. Starner, H.N. McManus, An experimental investigation of free convection heat transfer from rectangular fin arrays, *J. Heat Transf.* 85 (1963) 273–278.
- [2] I. Tari, Passive cooling assembly for flat panel displays with integrated high power components, *IEEE Trans. Consum. Electron.* 55 (2009) 1707–1713.
- [3] I. Tari, F.S. Yalcin, CFD analyses of a notebook computer thermal management system and a proposed passive cooling alternative, *IEEE Trans. Compon. Packag. Technol.* 33 (2010) 443–452.
- [4] G. Mittelman, A. Dayan, A. Dado-Turjeman, A. Ullmann, Laminar free convection underneath a downward facing inclined hot fin array, *Int. J. Heat Mass Transf.* 50 (2007) 2582–2589.
- [5] I. Tari, M. Mehrtash, Natural convection heat transfer from inclined plate-fin heat sinks, *Int. J. Heat Mass Transf.* 56 (2013) 574–593.
- [6] A. Dayan, R. Kushnir, G. Mittelman, A. Ullmann, Laminar free convection underneath a downward facing hot fin array, *Int. J. Heat Mass Transf.* 47 (2004) 2849–2860.
- [7] F. Harahap, D. Setio, Correlations for heat dissipation and natural convection heat-transfer from horizontally-based, vertically-finned arrays, *Appl. Energy* 69 (2001) 29–38.
- [8] F. Harahap, H.N. McManus, Natural-convection heat transfer from horizontal rectangular fin arrays, *J. Heat Transf.* 89 (1967) 32–38.
- [9] C.W. Leung, S.D. Probert, M.J. Shilston, Heat exchanger design: thermal performances of rectangular fins protruding from vertical or horizontal rectangular bases, *Appl. Energy* 20 (1985) 123–140.
- [10] C.W. Leung, S.D. Probert, Heat-transfer performances of vertical rectangular fins protruding from rectangular bases: effect of fin length, *Appl. Energy* 22 (1986) 313–318.
- [11] C.W. Leung, S.D. Probert, Heat-exchanger design: optimal thickness (under natural convective conditions) of vertical rectangular fins protruding upwards from a horizontal rectangular bases, *Appl. Energy* 29 (1988) 299–306.



- [12] C.W. Leung, S.D. Probert, Heat-exchanger design: optimal length of an array of uniformly spaced vertical rectangular fins protruding upwards from a horizontal base, *Appl. Energy* 30 (1988) 29–35.
- [13] C.W. Leung, S.D. Probert, Heat-exchanger performance: effect of orientation, *Appl. Energy* 33 (1989) 235–252.
- [14] C.W. Leung, S.D. Probert, Thermal effectiveness of short protrusion rectangular, heat exchanger fins, *Appl. Energy* 34 (1989) 1–8.
- [15] M. Dogan, M. Sivrioglu, Experimental and numerical investigation of clearance gap effects on laminar mixed convection heat transfer from fin array in a horizontal channel-A conjugate analysis, *Appl. Therm. Eng.* 40 (2012) 102–113.
- [16] M. Mehrtash, I. Tari, A correlation for natural convection heat transfer from inclined plate-finned heat sinks, *Appl. Thermal Eng.* 51 (2013) 1067–1075.
- [17] ANSYS Fluent 12.0 Users manual, ANSYS, Inc., 2008.
- [18] Data provided by F. Harahap via mail post marked 16.8.2012.
- [19] E. Ozden, I. Tolj, F. Barbir, Designing heat exchanger with spatially variable surface area for passive cooling of PEM fuel cell, *Appl. Therm. Eng.* 51 (2013) 1339–1344.
- [20] Z.R. Williamson, D. Chuna, K. Kwonb, T. Leea, C.W. Squibba, D. Kim, Evaluation of fin structure effects on a heated air-breathing polymer electrolyte membrane (PEM) fuel cell, *Appl. Therm. Eng.* 56 (2013) 54–61.
- [21] S. De Schampheleire, P. De Jaeger, R. Reynders, K. De Kerpel, B. Ameal, C. T’Joen, H. Huisseune, S. Lecompte, M. De Paepe, Experimental study of buoyancy-driven flow in open-cell aluminium foam heat sinks, *Appl. Therm. Eng.* 59 (2013) 30–40.
- [22] W-B Ye, D-S Zhu, N. Wang, Numerical simulation on phase-change thermal storage/release in a plate-fin unit, *Appl. Therm. Eng.* 31 (2011) 3871–3884.
- [23] S.F. Hosseinizadeh, F.L. Tan, S.M. Moosania, Experimental and numerical studies on performance of PCM-based heat sink with different configurations of internal fins, *Appl. Therm. Eng.* 31 (2011) 3827–3838.
- [24] Laminar natural convection heat transfer and air flow in three-dimensional rectangular enclosures with pin arrays attached to hot wall, *Appl. Therm. Eng.* 31 (2011) 3189–3195.
- [25] X. Yu, J. Feng, Q. Feng, Q. Wang, Development of a plate-pin fin heat sink and its performance comparisons with a plate fin heat sink, *Appl. Therm. Eng.* 25 (2005) 173–182.

**Table 1** Optimum fin spacing values minimizing the base temperature for both horizontal orientations

| $Q_{in}$ (W) | Optimum Fin Spacing at Horizontal Orientation, $S_{opt}$ (mm) for $L=250$ mm |           |          |               |           |          |
|--------------|--|-----------|----------|---------------|-----------|----------|
|              | Downward Facing  |           |          | Upward Facing |           |          |
|              | $H=25$ mm  | $H=15$ mm | $H=5$ mm | $H=25$ mm     | $H=15$ mm | $H=5$ mm |
| 25           | 9.3  | 9.1       | 8.8      | 13.9          | 13.6      | 12.4     |
| 50           | 9.5  | 9.3       | 9        | 13.5          | 13.6      | 13.7     |
| 75           | 9.7  | 9.4       | 9.2      | 12.8          | 13.5      | 13.8     |
| 100          | 9.8  | 9.5       | 9.4      | 12.5          | 13.5      | 13.8     |
| 125          | 9.9  | 9.6       | 9.6      | 12.3          | 13.5      | 13.9     |

**Table 2** Absolute relative errors of literature data in  $Nu_S$  when Eq. (5) is used.

| Reference             | Data                | Geometric parameters of heat sink |                |              |                | Absolute percent relative error in $Nu_S$ |              |              |
|-----------------------|---------------------|-----------------------------------|----------------|--------------|----------------|---|--------------|--------------|
|                       |                     | $S$ (m)                           | $H$ (m)        | $L$ (m)      | $t$ (m)        | Min                                       | Max          | Avg          |
| S-M-H<br>[18]         | H1                  | <b>0.00635</b>                    | <b>0.00635</b> | <b>0.127</b> | <b>0.00127</b> | <b>11.70</b>                              | 21.79        | <b>16.14</b> |
|                       | H2                  | <b>0.00635</b>                    | <b>0.0127</b>  | <b>0.127</b> | <b>0.00127</b> | <b>17.71</b>                              | 26.82        | 24.12        |
|                       | H3                  | <b>0.00635</b>                    | <b>0.00381</b> | <b>0.127</b> | <b>0.00127</b> | <b>2.64</b>                               | <b>8.81</b>  | <b>6.93</b>  |
|                       | H4                  | <b>0.00795</b>                    | <b>0.00254</b> | <b>0.127</b> | <b>0.00127</b> | <b>2.13</b>                               | <b>6.67</b>  | <b>4.30</b>  |
|                       | D1                  | 0.00635                           | 0.0131         | 0.1775       | 0.00127        | 29.56                                     | 87.15        | 58.07        |
|                       | D2                  | 0.00625                           | 0.0239         | 0.254        | 0.0031         | 30.47                                     | 90.70        | 82.39        |
|                       | D3                  | 0.00635                           | 0.0127         | 0.254        | 0.00102        | <b>14.85</b>                              | 75.79        | <b>20.28</b> |
|                       | D4                  | 0.0064                            | 0.00635        | 0.254        | 0.0031         | 30.33                                     | 68.27        | 44.39        |
|                       | D5                  | 0.00735                           | 0.0239         | 0.254        | 0.0023         | <b>20.38</b>                              | 74.20        | 35.99        |
|                       | P3/W1               | 0.00635                           | 0.00635        | 0.1765       | 0.00127        | <b>3.62</b>                               | 63.76        | 33.81        |
|                       | P4/W2               | 0.00635                           | 0.0131         | 0.1765       | 0.00127        | <b>20.59</b>                              | 31.37        | 25.69        |
|                       | S1                  | 0.00635                           | 0.00635        | 0.254        | 0.00102        | <b>20.80</b>                              | 86.69        | 31.30        |
|                       | S2                  | 0.00635                           | 0.0127         | 0.254        | 0.00102        | <b>14.85</b>                              | 77.31        | 59.23        |
|                       | S3                  | 0.00635                           | 0.0381         | 0.254        | 0.00102        | 45.94                                     | 77.31        | 70.84        |
|                       | S4                  | 0.00795                           | 0.0254         | 0.254        | 0.00102        | <b>20.38</b>                              | 74.20        | 64.41        |
|                       | Over all S-M-H data |                                   |                |              |                | 2.13                                      | 90.70        | 31.14        |
| L-P-S<br>[14]         | L1                  | 0.003                             | 0.17           | 0.15         | 0.003          | 45.95                                     | 61.51        | 53.73        |
|                       |                     | <b>0.006</b>                      | <b>0.17</b>    | <b>0.15</b>  | <b>0.003</b>   | <b>16.68</b>                              | 22.88        | <b>19.78</b> |
|                       |                     | <b>0.009</b>                      | <b>0.17</b>    | <b>0.15</b>  | <b>0.003</b>   | <b>6.70</b>                               | <b>10.59</b> | <b>8.64</b>  |
|                       |                     | <b>0.012</b>                      | <b>0.17</b>    | <b>0.15</b>  | <b>0.003</b>   | <b>5.43</b>                               | <b>9.88</b>  | <b>7.66</b>  |
|                       |                     | <b>0.015</b>                      | <b>0.17</b>    | <b>0.15</b>  | <b>0.003</b>   | <b>2.37</b>                               | <b>6.87</b>  | <b>4.62</b>  |
|                       |                     | <b>0.021</b>                      | <b>0.17</b>    | <b>0.15</b>  | <b>0.003</b>   | <b>2.18</b>                               | <b>9.09</b>  | <b>5.63</b>  |
|                       |                     | <b>0.03</b>                       | <b>0.17</b>    | <b>0.15</b>  | <b>0.003</b>   | <b>18.87</b>                              | 27.34        | 23.11        |
|                       |                     | 0.045                             | 0.17           | 0.15         | 0.003          | 37.74                                     | 44.19        | 40.96        |
|                       | L2                  | 0.003                             | 0.1            | 0.15         | 0.003          | <b>12.12</b>                              | 32.18        | 22.15        |
|                       |                     | <b>0.006</b>                      | <b>0.1</b>     | <b>0.15</b>  | <b>0.003</b>   | <b>1.48</b>                               | <b>6.89</b>  | <b>4.18</b>  |
|                       |                     | <b>0.009</b>                      | <b>0.1</b>     | <b>0.15</b>  | <b>0.003</b>   | <b>20.29</b>                              | 25.35        | 22.82        |
|                       |                     | <b>0.012</b>                      | <b>0.1</b>     | <b>0.15</b>  | <b>0.003</b>   | <b>17.97</b>                              | <b>17.97</b> | <b>17.97</b> |
|                       |                     | <b>0.015</b>                      | <b>0.1</b>     | <b>0.15</b>  | <b>0.003</b>   | <b>12.29</b>                              | <b>12.55</b> | <b>12.42</b> |
|                       |                     | <b>0.021</b>                      | <b>0.1</b>     | <b>0.15</b>  | <b>0.003</b>   | <b>5.01</b>                               | <b>5.25</b>  | <b>5.13</b>  |
|                       |                     | <b>0.03</b>                       | <b>0.1</b>     | <b>0.15</b>  | <b>0.003</b>   | <b>9.32</b>                               | <b>10.64</b> | <b>9.98</b>  |
|                       |                     | 0.045                             | 0.1            | 0.15         | 0.003          | 28.39                                     | 29.14        | 28.77        |
| Over all L-P-S data   |                     |                                   |                |              | 1.48           | 61.51                                     | 17.97        |              |
| Over all present data |                     |                                   |                |              | 0.03           | 14.31                                     | 4.32         |              |

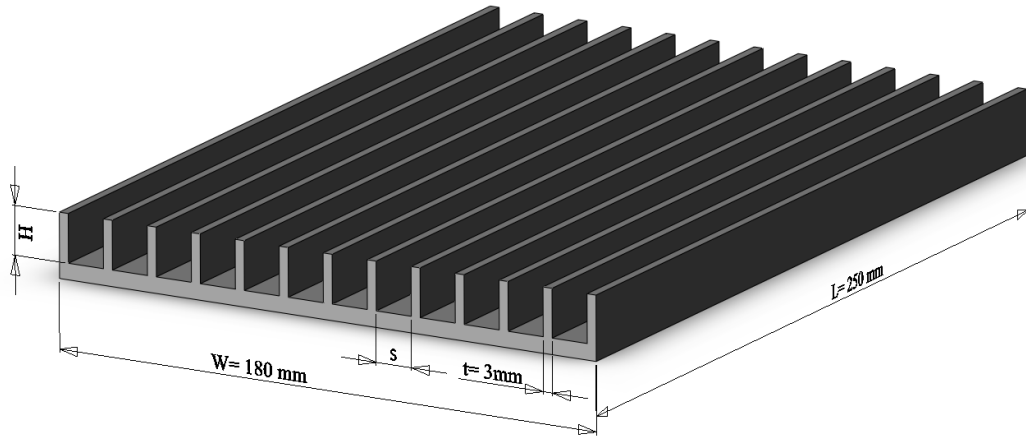


**Fig. 1.** Upward horizontal heat sink of  $L=250$  mm length and  $d=5$  mm base thickness (at  $-90^\circ$  inclination angle from vertical).

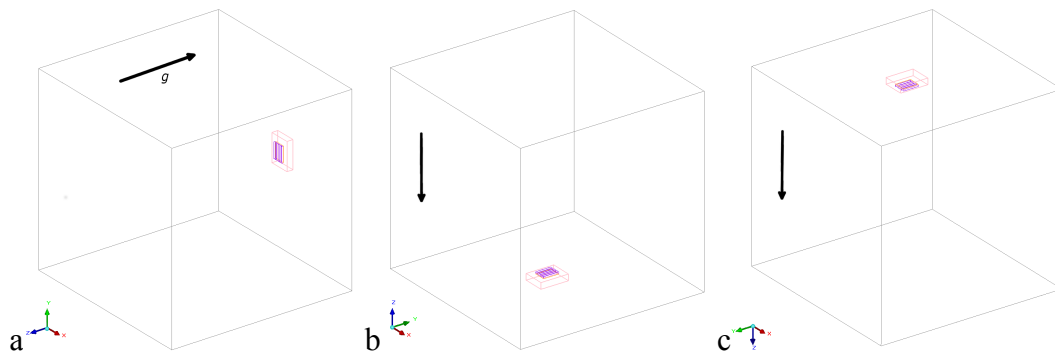


**Fig. 2.** (a) Vertical model is shown together with the gravitational acceleration vector creating the net effect of an upward facing horizontal heat sink that is shown in (b); downward facing horizontal heat sink in (c).

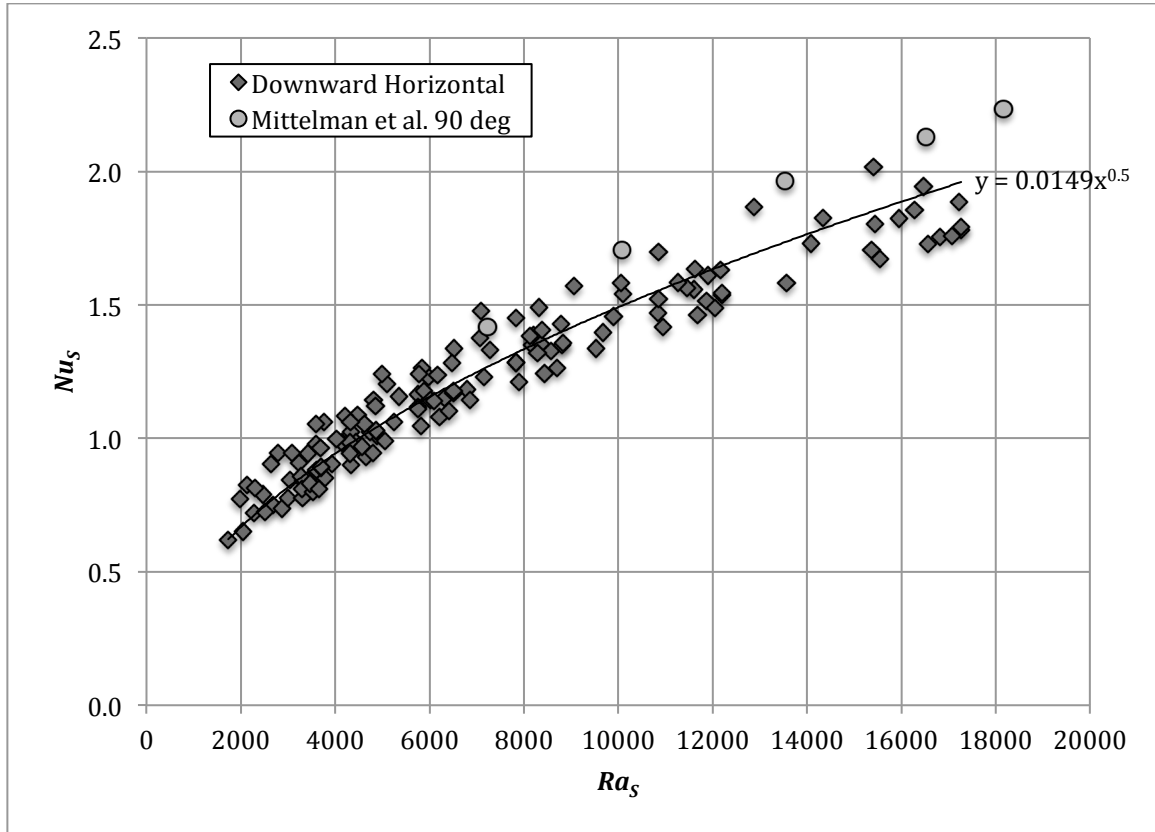


**Fig. 3.** Downward horizontal data plotted using suggested dimensionless groups to obtain Eq. (4) together with the downward horizontal data from Mittelman et al. [4].

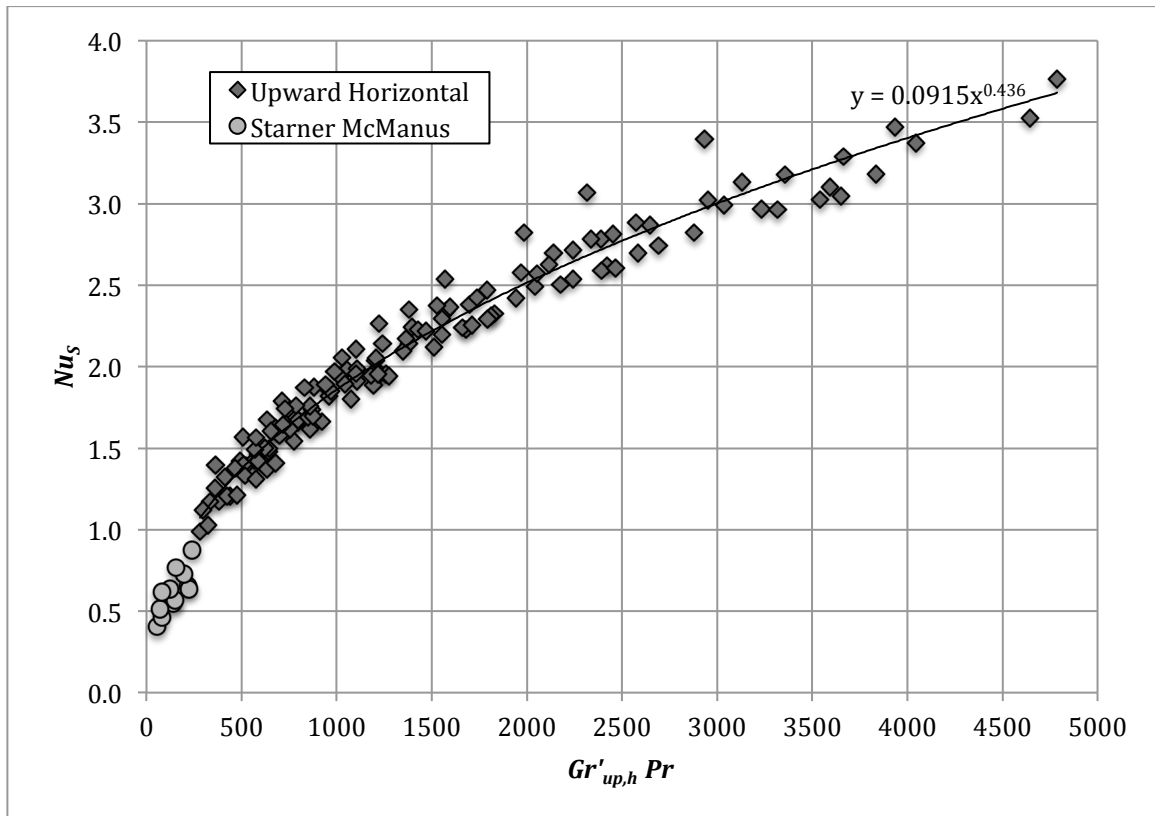


**Fig. 4.** Upward horizontal data plotted using suggested dimensionless groups to obtain Eq. (5) together with the data from Starner and McManus [1].

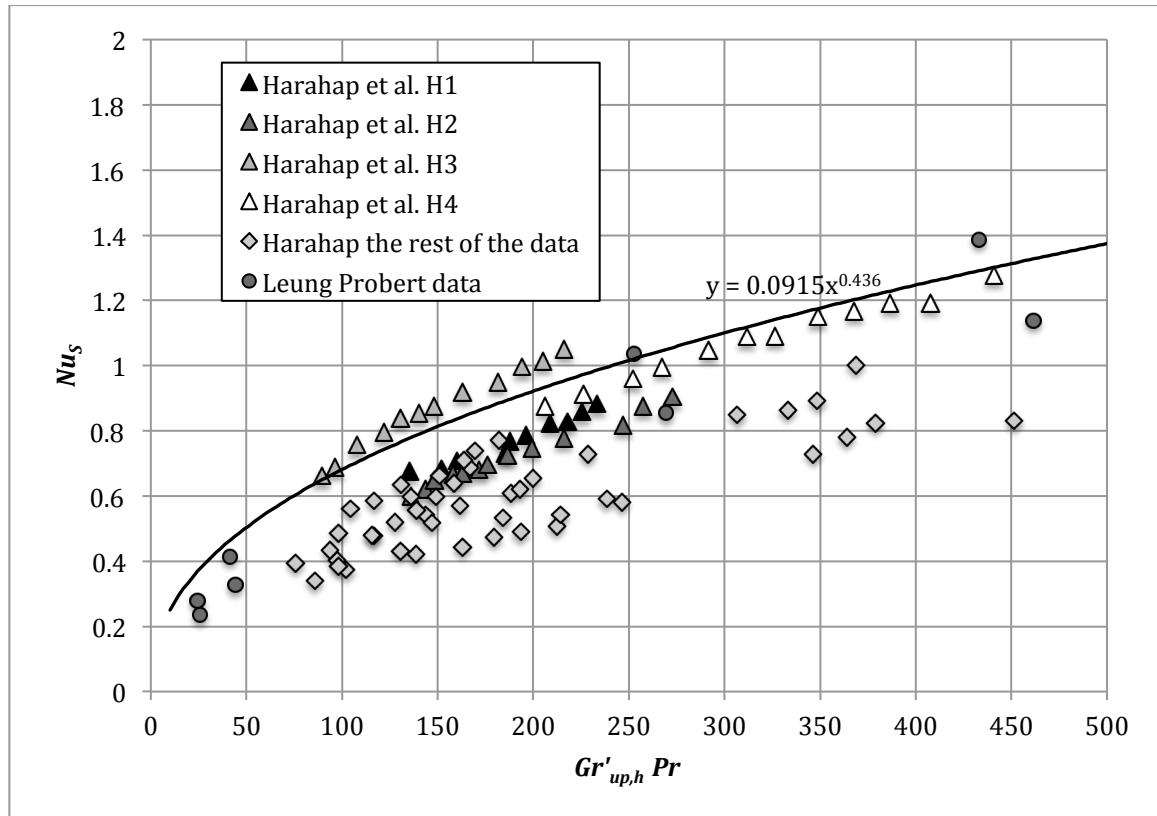


**Fig. 5.** Comparison of upward horizontal data with S-M-H [18] and L-P-S [14] data sets from literature.

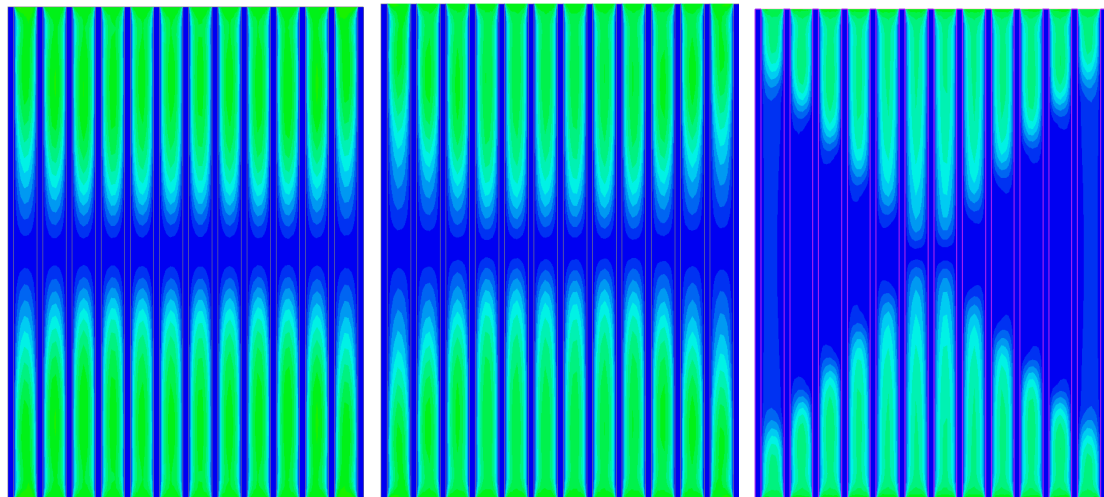


**Fig. 6.** Speed contours for the upward facing horizontal heat sinks of 25, 15 and 5 mm fin heights (from left to right) for  $Q_{in}=125$  W and  $L=250$  mm, and  $S=11.75$  mm, obtained at 2 mm above the base-plate surface. Vertical lines are the fins with 3 mm thickness. Darker colors (blue) show slower speeds.

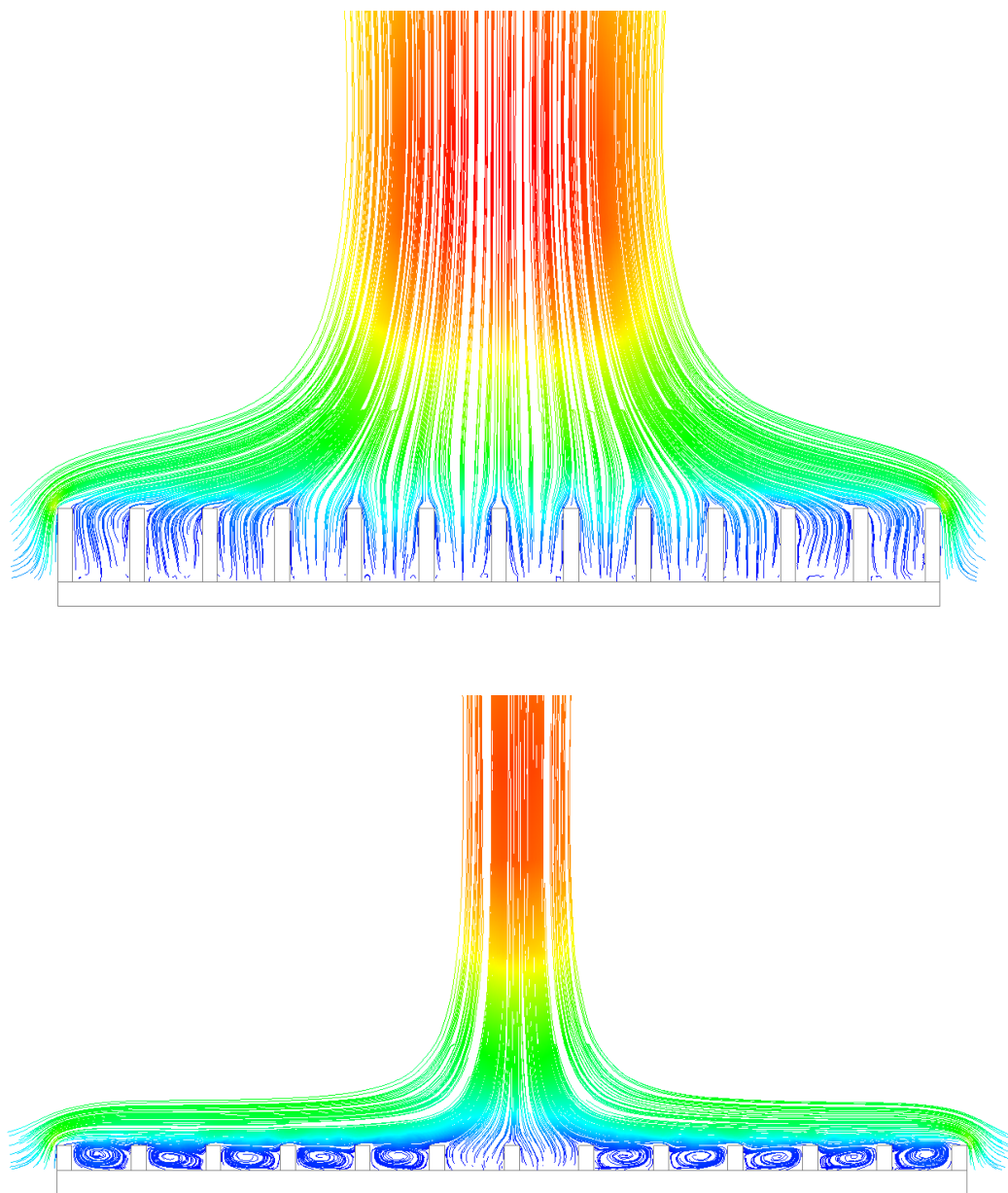


**Fig. 7.** Chimney flow structures at the mid-planes of the upward facing horizontal heatsinks with 15 mm (top) and 5 mm (bottom) fin heights. Note the longitudinal vortices in the flow channels of the 5 mm high fins.  $Q_{in}=125$  W and  $L=250$  mm, and  $S=11.75$  mm.

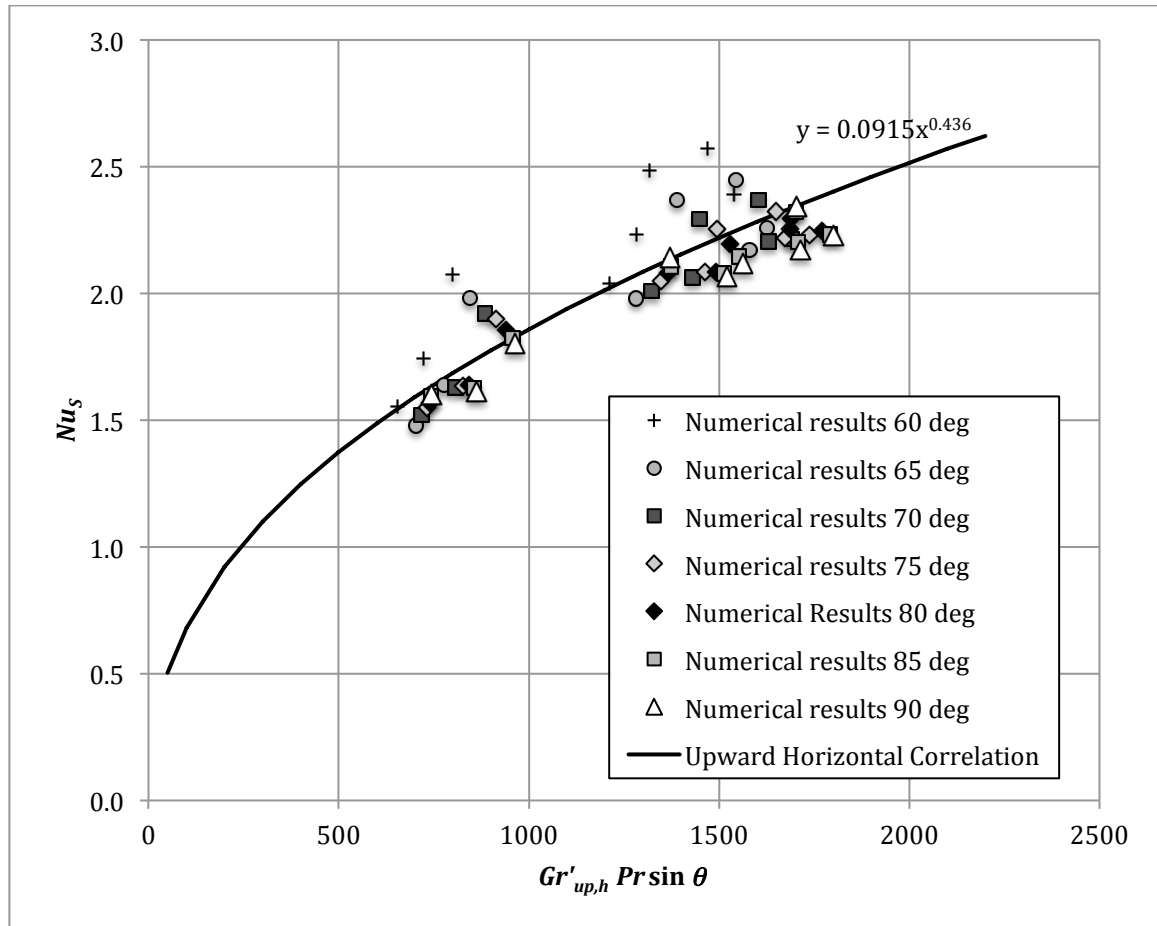


**Fig. 8.** Data for upward inclined close to horizontal inclinations in the  $-90^\circ < \theta < -60^\circ$  interval for  $S=11.75$  mm and  $L=250$  mm.



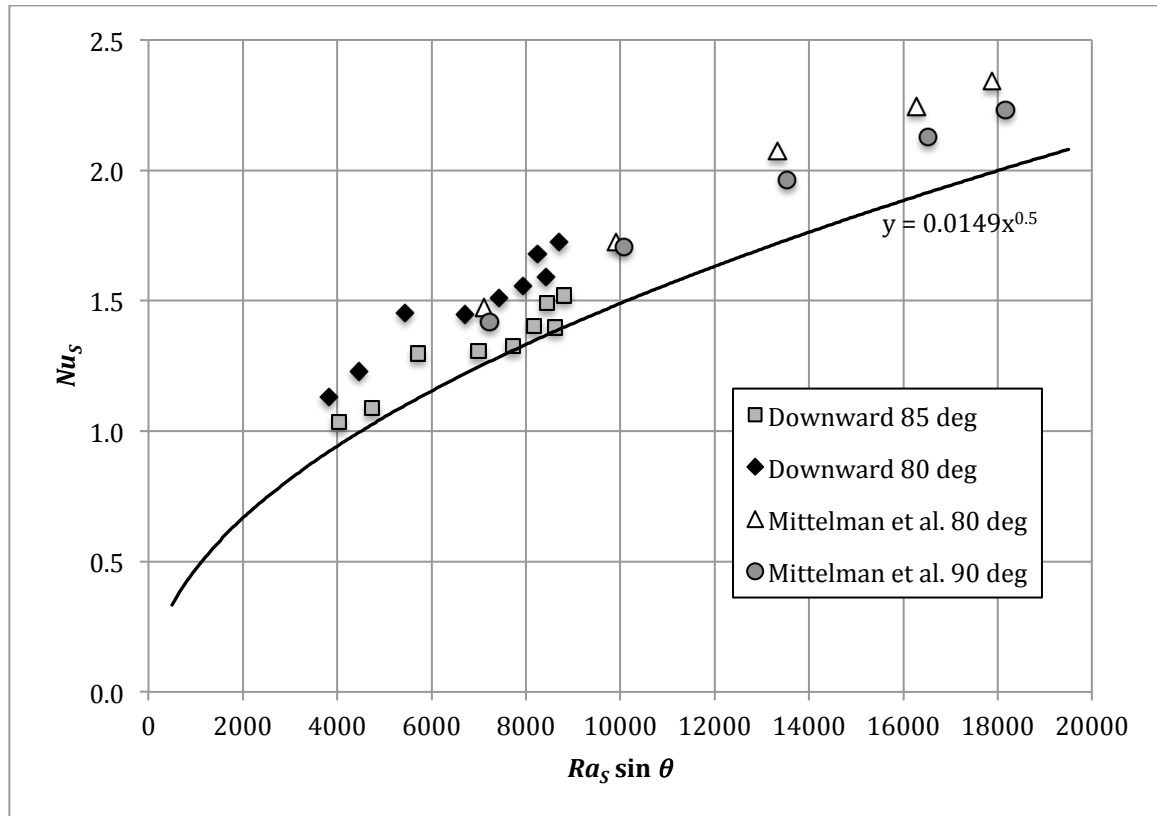


Fig. 9. Data for downward +85° and +80° inclinations together with Mittelman et al. [4] data.